ATOM INTERFEROMETRY IN A BOSE–EINSTEIN CONDENSATE RATCHET

By

AMRUTHAA SUNDARARAJ

Bachelor of Technology in Nanotechnology

SRM University

Chennai, India

2015

Submitted to the Faculty of the
Graduate College of the
Oklahoma State University
in partial fulfillment of
the requirements for
the Degree of
MASTER OF SCIENCE
May, 2018

ATOM INTERFEROMETRY IN A

BOSE–EINSTEIN CONDENSATE RATCHET

Thesis Approved by:

Dr. Gil Summy

Thesis Adviser

Dr. Albert T Rosenberger

Dr. Kaladi S Babu

ACKNOWLEDGEMENTS

I would like to begin by thanking my academic advisor, Dr. Gil Summy, for, first, letting me be a part of his group at Oklahoma State University. My passion for optics and experimental physics was only ever encouraged. My time in the lab has been a great learning experience.

I would also like to thank the members of my advisory committee, Dr. Rosenberger and Dr. Babu, for their comments and questions. Dr. Rosenberger has been a part of my graduate studies from day one and has been of tremendous help in all aspects from the choice of courses to the typos in my thesis. I am indebted to Dr. Siamak Dadras, my friend and lab mate, for guiding me with the experiment and clarifying all of my doubts.

The staff of the Department of Physics at Oklahoma State University, Susan Cantrell, Melissa Edwards, Alisha Leach, Beth Bridenstine and Tamra Raymond, have been very kind to me during my stay in Stillwater. I appreciate their efforts in helping me through any dilemma and for supporting me through the years.

Everything I am is because of the continual encouragement of my parents and no amount of gratitude expressed would ever be enough. All of my accomplishments are a result of their unwavering trust and undying support. I would also like to mention my many thanks to Emellia Roy for being my friend and family in good times and bad. Lastly, I thank Ashwin Venkatesan for accepting nothing less than excellence.

I look forward to everything life has to offer. Thank you.

Name : AMRUTHAA SUNDARARAJ

Date of Degree : MAY, 2018

Title of Study : ATOM INTERFEROMETRY IN A BOSE–EINSTEIN CONDENSATE RATCHET

Major Field : PHYSICS

Abstract : Interferometry is at the heart of all precision measurements. Atoms, like light, exhibit wave-like properties which makes it possible to construct an atom interferometer. The major optical elements essential to an interferometers are used to separate the stream of particles into two diverging atom waves, to bring them back towards each other and third to make them interact with each other. These atom optics are implemented experimentally by pulses of finely tuned light. Atom interferometry is achieved in ultra-cold ^{87}Rb by realizing a ratchet and reversing it. A $\pi/2$ microwave pulse is used as a beam splitter to split the atoms into two internal states and ratchet steps are carried out to take the two atom waves apart and to bring them back together. Another $\pi/2$ microwave pulse is used to make the two beams interact with each other to be able to observe an interference pattern. The interference is illustrated by the change in the population of the final states.

TABLE OF CONTENTS

LIST OF FIGURES

CHAPTER I

1. INTRODUCTION

1.1. Interferometer

An interferometer, or more specifically an optical interferometer, is an instrument that interferes two beams of light to create an interference pattern to make accurate measurements. Light from a single source is split into two beams and allowed to travel in different optical paths. The beams are then made to interfere to form the said pattern. The interference pattern carries information about the light and the path that the beam has travelled. Light beams of the same frequency mix when combined at a point. The variation in the interference pattern is mainly due to the difference in phase acquired by the two beams in their respective paths. When the waves are in phase with each other, they will undergo a constructive interference pattern and when they are out of phase with each other, they will undergo a destructive interference pattern. When the waves are not completely in phase with each other or completely out of phase with each other, the intensity of the interference pattern would be an intermediate between the maximum and minimum intensity. The relative phase difference can then be calculated based on the intensity of the interference.

There are various types of interferometers based on the property they measure such as field, intensity and quantum behavior or based on the type of waves they use. One such interferometer configuration is the Mach-Zehnder Interferometer. This interferometer works on the principle described above where light from a single collimated source is split and the phase difference accumulated in the different path is measured.

Figure 1 illustrates the path travelled by the beams of light in a Mach-Zehnder interferometer. Light from a collimated source is split into two beams by beam splitter 1 and then the light beams are each reflected by respective mirrors and then combined and interfere at beam splitter 2, which can then be detected by photodiodes 1 and 2 respectively.

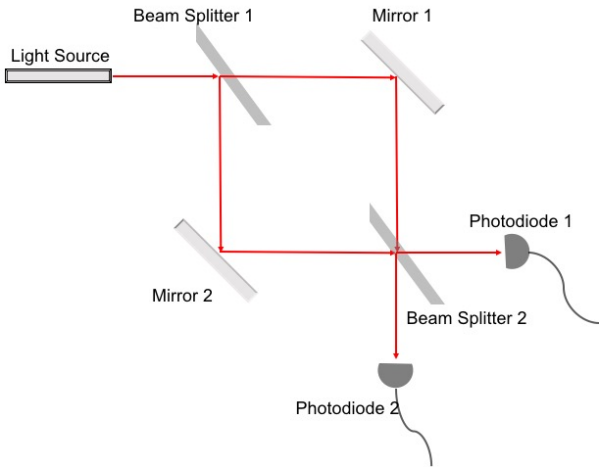

Figure 1: Mach-Zehnder Interferometer

Fresnel equations describe the reflection and transmission of waves by a dielectric coated surface. This is followed by the mirrors as well as dielectric coated beam splitters. The phase acquired by the two beams arriving at photodiode 1, in this particular schematic, is exactly the same owing to their optical paths (the beams have undergone one transmission and two reflections). Hence, constructive interference is observed at photodiode 1. On the other hand, the phase acquired by the two beams arriving at photodiode 2 is different by 180° (or half a wavelength) and hence, destructive interference will be observed (no light will be observed). Usually, a sample material is placed in the optical path of one of the beams such that they acquire a certain phase such that the intensities of the beams entering the two photodiodes will change. This allows for the calculation of phase shift caused by the sample in comparison to the reference beam (without the sample).

The resulting interference pattern in an interferometer can be used to calculate the optical path difference between the two beams. The accuracy of the measurements depends on the wavelength of the light used, which makes interferometers one of the most precise instruments to measure length. The Mach-Zehnder interferometer configuration is a popular configuration for holography interferometry and for various quantum entanglement studies like single photon interferences.

1.2. Atom Interferometer

Interference is a phenomenon that can be observed for all waves. Matter exhibits wavelike behavior under certain conditions and under those conditions, interference of atom waves can be observed. An atom interferometer needs to manipulate the translational motion of atoms coherently. The atom waves are selectively pushed towards their respective paths and then recombined spatially to see the interference pattern. This requires mechanisms to manipulate the atom waves similar to how the light waves can be manipulated with optical elements. The basic steps towards achieving atom interferometry is as follows:

- Preparing coherent initial states of the atom waves
- Splitting the atom waves into two or more states in position
- Apply differing interactions to the different states
- Recombine the different states in position
- Measure the difference in phase shift of the interference

The uncertainty principle states that both the position and momentum of a quantum system cannot be known at the same time. Spatial delocalization is caused due to the momentum uncertainty when free atoms are localized in position space. Hence, by reducing the momentum of a group of atoms by laser cooling and trapping, the atoms can be trapped in a small volume. Laser cooling has been described as a technique analogous to the optical pumping for internal states. In fact, cooling atoms in a trap is even more exactly analogous to optical pumping because trapped atoms are in discrete translational states and can ultimately be prepared in the single ground state[1].

Interference of atom waves require manipulation of the atoms and development of atom optics that will act as the beam splitters and mirrors affecting the translational motion of atoms.

Difficulties arise because, atoms stick to surfaces, are only weakly affected by electric fields, and do not propagate very far in solid crystals [2]. Nevertheless, a variety of beam splitters are available for coherent manipulation of the de Broglie waves of the atoms including laser pulses, standing waves of light, nanogratings and magnets. For example, when using light pulses, a Raman transition can be used to split the atoms into a coherent superposition of momentum orders. Once the split "beams" are sufficiently far apart, different interactions can be applied or measured to them separately to change the phase of the atom waves so that they interfere when recombined. The recombination can be achieved by using another Raman transition. Interference fringes are observed due to the difference in phase.

The output of this type of interferometer can be observed by state selective detection of the number of atoms in the internal state. The number of atoms in the 2 states will oscillate with respect to the phase acquired by the two beams. This is analogous to the Mark-Zehnder interferometer.

Although, many parallels can be drawn between the techniques of optical interferometry and atom interferometry, there are a few significant differences. The de Broglie wavelengths of matter waves are very short (~10 pm for thermal atoms and ~10 μm for ultra-cold atoms[1]). They also have very short coherence lengths. This requires that the period and the position of the interference fringes must be independent of the de Broglie wavelength of the incident atoms. This is observed in white light interferometry where the waves are coherent for short length and time scales. Perhaps a more significant difference between optical and atom interferometry is that the atoms may interact with each other and their behavior is often nonlinear. Also, the atoms may be confined throughput the entire interferometer and this is unheard of in optical interferometers. It is interesting to note that in optical interferometry, matter is used to manipulate the propagation and in atom interferometry, light is used to manipulate the propagation of atom waves.

1.3. Bose Einstein Condensate

Statistical mechanics describes particle statistics in order to define multiple particles. Maxwell–Boltzmann statistics characterizes distinguishable classical particles. Quantum mechanics, on the other hand, defines and classifies indistinguishable particles in two categories depending on their spin. Particles having half integer spins are called fermions and defined in the Fermi–Dirac statistics and particles having integer spins are called bosons and defined in the Bose–Einstein statistics. All quarks, leptons, and composite particles made of odd numbers of quarks and leptons are fermion, and photons, gluons and nuclei having even mass numbers are bosons. Fermions and bosons further differ in the occupation statistics. Pauli's exclusion principle states that two or more fermions cannot occupy the same quantum state in a quantum system simultaneously, where as there is no such restriction for bosons. This makes Bose–Einstein condensates a possibility, where a gas of bosons is cooled by reducing its kinetic energy such that they condense into the lowest energy state. Bose Einstein Condensates are of much interest as they exhibit quantum behavior at macroscopic scales. The atoms start exhibiting wave like characteristics as their temperature is reduced due to the wave-particle duality. By further cooling the atoms below the critical temperature, we can observe a Bose–Einstein condensate where the wave functions of the atoms superimpose such that all of the atom confined in the trap are indistinguishable.

The distribution function for bosons in the Bose–Einstein statistics is given as follows,

$$N = \sum_{k} \frac{1}{e^{\beta'(\epsilon_k - \mu)} - 1} \tag{1.3.1}$$

where $\beta' = \frac{1}{k_B T}$, k_B is the Boltzmann constant, T is the temperature, μ is the chemical potential, k is the wave vector and N is the total number of bosons. In a thermodynamic limit where the volume V and N are large, the sum can be replaced with an integral as follows,

$$n = \frac{N}{V} = \frac{1}{(2\pi)^3} \int \frac{1}{e^{\beta'(\epsilon_k - \mu)} - 1} d^3k \tag{1.3.2}$$

where n is the number density. The chemical potential goes to zero if the temperature decreases for a constant n. By simplifying the equation, we get the following result,

$$n = 2.612 \left(\frac{M k_B T_C}{2\pi\hbar^2} \right)^{3/2} \tag{1.3.3}$$

The critical temperature or the transition temperature is given as,

$$T_C = \frac{3.31\ \hbar^2}{M k_B}\ n^{3/2} \tag{1.3.4}$$

For temperatures lower than the critical temperature, some fraction of bosons condenses to the lowest energy state. The de Broglie wavelength is defined as follows, and the number density can be written in terms of the phase density which turns out to be a constant from Eq. (1.3.3).

$$\lambda_{dB} = \frac{\hbar}{\sqrt{2\pi M k_B T}} \tag{1.3.5}$$

$$\rho = n\lambda_{dB}^3 \cong 2.612 \tag{1.3.6}$$

Condensation occurs when the phase density is equal to or more than 2.612. The phase density is directly proportional to the number of atoms and inversely proportional to the temperature. Experimentally, the atoms are first cooled down to several hundred micro Kelvin by optical molasses and then further cooled by evaporative cooling (EVC).

1.4. Brownian Ratchet

Also known as the Feynman-Smoluchowski ratchet, a Brownian ratchet is a thought experiment that allows the apparent perpetual motion of a ratchet driven by the Brownian motion. It was first analyzed by Marian Smoluchowski and then popularized by Richard Feynman. In this experiment, a paddle wheel and a ratchet are connected such that the system can extract useful work from random thermal fluctuations. This is in violation of the second law of thermodynamics. The second law states that the entropy of an isolated system will always increase. There are different ways of stating the second law, the one that applies here is, "It is impossible for any device that operates on a cycle to receive heat from a single reservoir and produce a net amount of work."

The device, shown in Figure 2, is a ratchet that rotates freely in one direction but cannot move in the opposite direction as it is restricted by the pawl. The ratchet is connected to a paddle wheel by an axle. The molecules surrounding the paddle wheel is at temperature T_1 and those around the ratchet at temperature T_2. The device is light and small enough to be affected from impulses from molecular collisions. Since molecular collisions are random, the wheel can turn in any direction, but the pawl in the ratchet end allows for rotation in one direction only. It may seem like after many random collisions, the ratchet may continuously rotate in one direction. This motion can then be used to do useful work, such as raising a weight against gravity. The energy necessary to do this work, comes from the heat at around the paddle wheel.

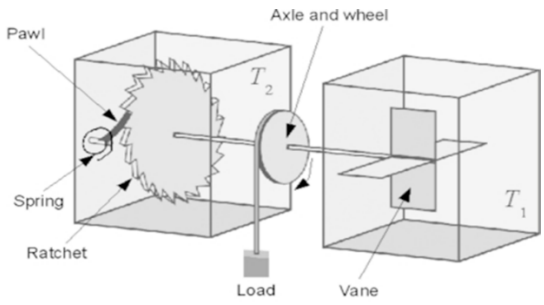

Figure 2: Brownian Ratchet [3]

However, this is not a complete picture. If the entire device is maintained at the same temperature, due to Brownian motion, the pawl will also will bounce up and down. As a result, the ratchet will not just move in one direction but randomly in both directions. This in turn means that no net useful work will be produced. Another part of the system is the spring that holds the pawl. As the spring exerts a sideways force on the side of the ratchet that the pawl is resting on, the ratchet tends to rotate in the backward direction. If $T_1 = T_2$, failure rate of the ratchet moving backward is the same as the rate of the ratchet moving forward and so no net motion happens over time.

If $T_1 > T_2$, the ratchet will move forward and useful work can be extracted. But this is due to the temperature gradient of the two reservoirs and the cooler reservoir T_2 is ever so slightly heated due to the random motion of the pawl. This is a model of the conventional heat engine and follows the second law of thermodynamics.

This device is an example of Brownian motor, in which Brownian motion is used to move things in a particular way and extract useful work. The devices are nano-scaled or molecular. In fact, biological protein-based molecular motors are thought to be Brownian motors. An example is the F0F1 ATPase that converts chemical energy to mechanical energy.

1.5. Quantum Resonance Ratchet

Classical ratchets require dissipative energy to produce useful work [4]. A quantum ratchet on the other hand, is a Hamiltonian ratchet and has no classical analog. It is manifested by a directed current of particles in the absence of net bias force and has been extensively studied [6, 7, 8]. A quantum system, such as a Bose–Einstein condensate, is a plane wave in the position space, i.e. the atoms are delocalized. However, by performing a Fourier transform, it is seen that the momentum space distribution of the BEC is a delta function as all the atoms in the BEC have the same momentum. Hence, the system in position experiences no net force due to a sinusoidal periodic potential. But with two or more such coherent systems, the position space distribution is not a plane wave. The effect of the periodic potential will still be zero as the initial distribution is still symmetric with the distribution. As a result, the ratchet doesn't move. Hence, by making a non-symmetric alignment of the atomic state and the periodic potential, the ratchet effect is observable. The atoms experience a net force due to a potential gradient in the direction of the gradien. This is illustrated in Figure 3.

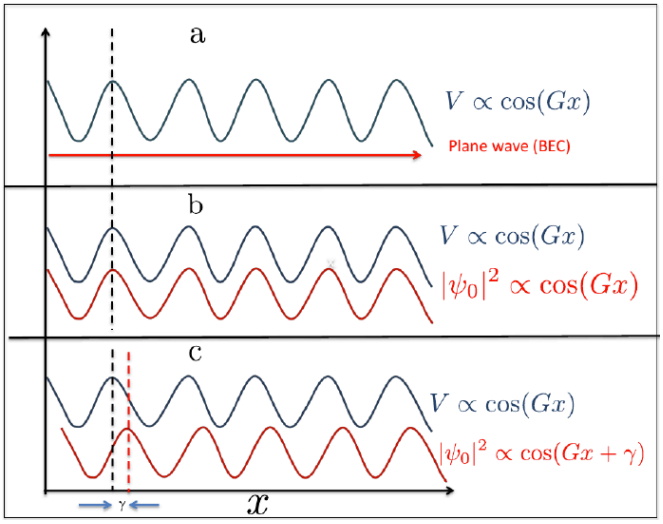

Figure 3: Quantum ratchet effect. The periodic potential is illustrated in blue and the atomic distribution in red. The ratchet effect is not observed in (a) and (b) due to the alignment of the symmetry centers. Directed motion to the right is observed in (c) due to the potential gradient observed by the atoms [4]

CHAPTER II

2. LASER COOLING AND TRAPPING

The idea of laser cooling and trapping originates from light – matter interaction and the consequent force on the atom caused due to the scattering of photons. The scattering force is proportional to the scattering rate and the momentum of the photon being absorbed. The momentum imparted due to an absorbed photon is much lower than the atomic velocity. But considering the substantial number of such absorptions occurring when a laser of sufficient intensity is focused at a group of atoms, the force slows down the atoms in motion. The average force on a stationary atom is defined as the expectation value of the quantum mechanical force operator, which is the negative gradient of the Hamiltonian. The optical force on a stationary two level atom is derived in [4] and is defined as,

$$F = \pm \frac{\hbar k \gamma s}{2\left[1 + \left(\frac{2\delta}{\gamma}\right)^2 + s\right]} \tag{2.1}$$

where $\hbar k$ is the photon momentum, γ is the spontaneous emission rate, δ is the detuning of the laser frequency to that of the atomic transition, and s is the saturation parameter. The $\pm$ indicates the force felt by atoms moving along or in the opposite direction of the light field respectively. It is noted that the force is defined in terms of a detuned laser. An atom moving in the direction of the laser will see a Doppler shifted frequency, depending on if the atom is moving in the direction of laser propagation or in the opposite direction of propagation of the laser propagation.

The atoms moving with velocity v, along the direction of the laser, will see a detuning of $\delta - kv$ and the atoms moving in the opposite direction of the laser will see a detuning of $\delta + kv$. In each absorption event, the atom loses some energy. Hence, the optical force on a moving atom can be written as,

$$F = \pm \frac{\hbar k \gamma s}{2\left[1 + \left(\frac{2(\delta \mp kv)}{\gamma}\right)^2 + s\right]} \tag{2.2}$$

Now if we have a configuration where there are counter-propagating beams, both the atoms moving along and in the opposite direction of the laser propagation can be addressed and the net force felt by the atom would be,

$$F = \frac{\hbar k \gamma s}{2\left[1 + \left(\frac{2(\delta - kv)}{\gamma}\right)^2 + s\right]} - \frac{\hbar k \gamma s}{2\left[1 + \left(\frac{2(\delta + kv)}{\gamma}\right)^2 + s\right]} \tag{2.3}$$

The equation for force results in a velocity (v) dependent force, in the condition that the Doppler shift is small compared to the detuning, $F = -\beta v$, where β is the dampening coefficient given by,

$$\beta = \frac{8\hbar k^2 s \delta}{\gamma\left[1 + \left(\frac{2\delta}{\gamma}\right)^2 + s\right]^2} \tag{2.4}$$

Let's consider a case where the laser frequency is red–detuned or detuned below the transition frequency ($\delta < 0$). For atoms that are moving in the same direction as the photons, the frequency is red shifted (sees lower frequency and hence, lower energy) and so the atoms do not interact. For atoms that are moving in the opposite direction of the laser, the light is blue detuned and so it absorbs photons more efficiently. This excited electron spontaneously emits a photon in a random direction. This dampening mechanism is called optical molasses. By having three pairs of counter propagating beams, velocity components in all three directions can be slowed down.

The cooling works on the principle of momentum conservation. It may seem like this process can cool the system down to absolute zero but the cooling is limited by the heating due to the spontaneous emissions (recoil heating). When the recoil heating rate equals the cooling rate of the optical molasses, a steady state is reached. This limits the cooling to the Doppler temperature. Mathematically, the Doppler temperature is given as,

$$T_D = \frac{\hbar\gamma}{2k_B} \tag{2.5}$$

For Rubidium-87, the Doppler temperature is about 146 μK [4]. Remarkably, a lower Doppler limit was observed [9]. It was later understood that multiple atomic transitions that were not considered and that could have been playing a role in this sub-Doppler cooling [10, 11].

The final characteristic temperature associated with laser cooling is the photon recoil limit. This temperature corresponds to the energy associated with the single photon recoil. In the process of absorption or emission of photons, the atoms obtain a recoil velocity $v_r = \frac{\hbar k}{m}$. The corresponding temperature is called the recoil limit and is defined as,

$$T_r = \frac{\hbar^2 k^2}{2mk_B} \tag{2.6}$$

For Rubidium-87, the recoil limit is 360 nK [4].

2.1. Magneto-Optical Trap

Optical Molasses is strictly velocity dependent and as a result, the atoms can diffuse out of the system. By introducing a spatially varying magnetic field (realized by a set of anti–Helmholtz coils), a position dependent force can be established. A magneto-optical trap (MOT) is used to trap and cool neutral atoms using an inhomogeneous magnetic field and pairs of counter

propagation red-detuned laser beams. Figure 4 shows the behavior of the hyperfine states in an inhomogeneous magnetic field.

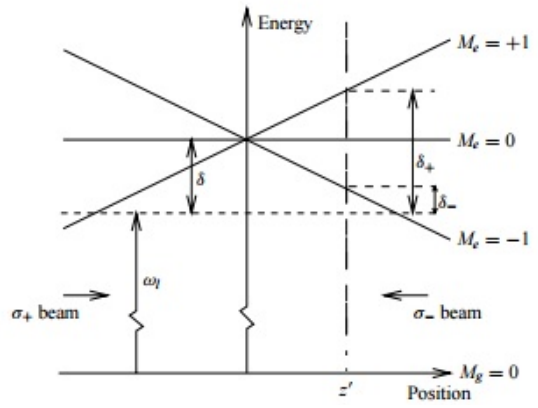

Figure 4: Arrangement for a MOT in 1D. The horizontal dashed line represents the laser frequency seen by an atom at rest in the center of the trap. Because of the Zeeman shifts of the atomic transition frequencies in the inhomogeneous magnetic field, atoms at z = z' are closer to resonance with the σ− laser beam than with the σ+ beam, and are therefore driven toward the center of the trap [12].

Consider a transition from ground state $J_g = 0$ to excited state $J_e = 1$ in a spatially varying magnetic field $(B = B(z) = B_o z)$. The excited state has three Zeeman components corresponding to $M_e = 0, \pm 1$. The $M_e = +1$ is shifted up for $B > 0$, whereas the state with $M_e = -1$ is shifted down. This shift is reversed for $B < 0$. At position z' $(B > 0)$ in Figure 4, the magnetic field therefore adjusts the $\Delta M = -1$ transition closer to resonance and the $\Delta M = +1$ transition further out of resonance. If the polarization of the laser beam incident from the right is chosen to be σ_- and correspondingly σ_+ for the other beam, then more light is scattered from the σ_- beam than from the σ_+ beam. Thus the atoms are driven toward the center of the trap where the magnetic field is zero. On the other side of the center of the trap, the roles of the $M_e = \pm 1$ states are reversed and now more light is scattered from the σ_+ beam, again driving the atoms towards the center.

The process of cooling atoms in a MOT is very similar to the cooling process in Doppler Cooling. Additionally, trapping takes place due to the interplay between the inhomogeneous magnetic field

and the cooling light. In addition to the velocity of the atoms, the detuning of the laser frequency from the transition frequency now depends on the magnetic field gradient. Mathematically,

$$\delta_{\pm} = \delta \mp \vec{k}.\vec{v} \pm \frac{\mu' B}{\hbar} \tag{2.1.1}$$

Where $\mu' = \mu_B(g_e M_e - g_g M_g)$ is the effective magnetic moment, μ_B is the Bohr magneton and g is the Landé g-factor. Hence, the force on the atom becomes,

$$F = \pm \frac{\hbar \vec{k} \gamma s}{2\left[1 + \left(\frac{2\delta_{\pm}}{\gamma}\right)^2 + s\right]} \tag{2.1.2}$$

A MOT is a very popular trap owing to its relatively easy experimental setup. It does not depend on the precise balancing of the optical trap and uses a magnetic field gradient that can be achieved by using simple, air-cooled coils in the anti-Helmholtz configuration. While, this is only for the atoms in 1 D, it can be extended 3D by using three pairs of counter propagating laser beams in the three orthogonal directions.

2.2. Evaporative cooling

As mentioned earlier, reducing the temperature is not enough to observe a BEC. In order to do so, the phase space density, $\rho = n\lambda_{dB}^3$, should be greater than 2.612, where n is the density and λ_{dB} is the de Broglie wavelength of the atom. With a MOT and optical molasses, the phase space density is increased to $10^{-5} - 10^{-4}$. Thermal atoms at room temperature at typical densities of 10^{10} atoms/cm^3, the phase space densities are of the order 10^{-17} [17]. With laser cooling, we can confine and reduce the temperature of the gas without much loss in the number of atoms, thus, increasing the density of the gas. This increases the number of collisions between atoms in

ground state and excited state. These collisions are inelastic and lead to further heating of the atoms. Therefore, near-resonant light is not preferred to achieve a condensate.

The concept of evaporative cooling is to preferentially remove atoms with higher energy from the trap followed by the rethermalization of atoms through elastic collisions. As both temperature and volume decrease, the phase space density increases. A Far Off-Resonant Trap or a Dipole trap creates an attractive or repulsive potential, if it's red or blue detuned from the atomic transitions respectively.

When the FORT laser is turned on, the electric field of the laser induces a dipole moment, μ, on the atoms that then interact with the electric field of the radiation. In the case of Rubidium-87 when a CO_2 laser is used, an attractive potential is created. This potential is given by,

$$U = -\frac{1}{2} a_g E^2 \tag{2.2.1}$$

where a_g is the ground state polarizability of the atoms and E is the electric field. For a Gaussian beam in z-direction, the trapping potential is given by,

$$U \approx -\frac{1}{2} a_g E^2 \left(1 - \frac{2x^2}{w_o^2} - \frac{2y^2}{w_o^2} - \frac{z^2}{z_R^2}\right) \tag{2.2.2}$$

where w_o^2 is the beam waist and z_R is the Rayleigh range. The depth of the trap is inversely proportional to the detuning of the laser from the atomic transition, whereas the spontaneous scattering rate is inversely proportional to the square of detuning. Therefore, to achieve an efficient evaporative cooling it is preferable to use a laser with a large detuning because the scattering rate will drop faster than the potential depth as the detuning is increased.

CHAPTER III

3. HAMILTONIAN RATCHETS

3.1. Atom Optic Quantum Delta Kicked Rotor

Quantum resonance ratchets have been used to study the crossovers between classical and quantum behavior [6, 7, 8, 13]. A quantum ratchet produces a directed currents of atoms and is implemented by an atom optic kicked rotor (AOKR). A quantum delta kicked rotor is realized using ultra cold atoms and a series of short pulses of a one dimensional off-resonant optical lattice called kicks. The Hamiltonian describing the AOKR is,

$$\widehat{H} = \frac{\hat{P}^2}{2M} + \hbar\phi_d\left[1 + cos\,(G\hat{X})\right]\sum_{j\in Z}\delta(t - jT) \tag{3.1.1}$$

where $\hat{P}$ is the momentum and M is mass of the particle, $\hat{X}$ is the position, and G is the grating wave-vector. The interference of the two counter propagating waves of the optical lattices is given by the factor, $\left[1 + cos\,(G\hat{X})\right]$. δ represents the delta function representing the temporal periodicity of the kicks, j is the number of kicks with period T. The kicking strength is given by $\phi_d = \frac{\Omega^2\Delta t}{8\delta_L}$, where Ω, Δt, and δ_L is the Rabi frequency, pulse length, and detuning of the laser. The spatial period of the potential is given as $2\pi/G$ and only transitions between momentum that differ by integer multiples of the two photon recoil, $\hbar G$ are allowed. A Floquet operator defines the one period evolution of the rotor and is given by,

$$\hat{F} = \widehat{U}_{free}\widehat{U}_{kick} = e^{-i\frac{\hat{p}^2}{2}\tau}e^{-i\phi_d[1+cos(\hat{x})]} \tag{3.1.2}$$

where $\widehat{U}_{free}$ represents the free evolution of the atomic wave and $\widehat{U}_{kick}$ is the kick imparted by each pulse, $\hat{x} = G\hat{X}$, $\hat{p} = \hat{P}/\hbar G$ and τ is the scaled pulse period, $\tau = 2\pi\frac{T}{T_{1/2}}$ the scaled momentum. $T_{1/2} = \frac{2\pi M}{\hbar G^2}$ is defined as the half-Talbot time. The $e^{-i\phi_d}$ part of the operator introduces a global phase to the system due to each kick but the periodic part of the operator ($e^{-i\phi_d cos(\hat{x})}$) behaves like a thin phase grating. The evolution of the a wave function ($|\psi_j\rangle$) after a kicking pulse is given by,

$$|\psi_{j+1}\rangle = \widehat{U}_{kick}|\psi_j\rangle = e^{-i\phi_d[1+cos(\hat{x})]}\,|\psi_j\rangle \tag{3.1.3}$$

3.2. Quantum Resonance Ratchet

A picture of the ratchet mechanism can be developed from a consideration of the gradient of the standing wave, which serves as a driving force on the wave function of the atoms [7]. At positions of the highest gradient, by maximizing the intensity of the atom wavefunction, the ratchet mechanism is observed and the sign of the potential gradient determines the direction of the ratchet. As discussed in section 1.5, an initial state of two or more plane waves is to be created such that the wavefunction would be,

$$|\psi\rangle = \sum_n e^{-in\phi}|n\rangle \tag{3.2.1}$$

where $|n\rangle$ is the momentum state $|n\hbar G\rangle$ and ϕ is the offset phase. The gradient of the potential is maximum when $\phi = \pi/2$. In the position space, a BEC with more than one initial state can be written as,

$$\phi(x) = A\sum_n e^{in\phi}e^{ip_n x/\hbar} \tag{3.2.2}$$

where A is a normalization factor. Figure 3 illustrates how at the $\phi = \pi/2$ offset phase, the peaks of the population of the BEC atom wave is where the standing wave has the greatest gradient. To optimize the ratchet current, the initial state of the atom waves should contain a superposition of consecutive momentum states. It is seen that momentum states $|-1\rangle + |+1\rangle$ would be less optimal initial state than $|0\rangle + |+1\rangle$ [7]. Hence, the following initial states are chosen for the experiment,

$$|\psi\rangle = \frac{1}{\sqrt{2}}(|n=0\rangle + e^{in\phi}|n=1\rangle) \tag{3.2.3}$$

where $\phi = \pi/2$. The preparation of this initial state involves applying an off-resonant standing wave for 103 μs on the initial BEC with $|n=0\rangle$. The Bragg pulse couples the two momentum state with the following interaction matrix,

$$\hat{B} = \begin{pmatrix} \cos\left(\frac{\Omega_B t_B}{2}\right) & e^{i\phi_B}\sin\left(\frac{\Omega_B t_B}{2}\right) \\ -e^{i\phi_B}\sin\left(\frac{\Omega_B t_B}{2}\right) & \cos\left(\frac{\Omega_B t_B}{2}\right) \end{pmatrix} \tag{3.2.4}$$

where Ω_B is the effective Rabi frequency, t_B is the pulse length and ϕ_B is the offset phase for the Bragg pulse. Equal population in both states is achieved by choosing $\phi_B = \pi/2$ and adjusting the Rabi frequency of the standing wave such that $\Omega_B t_B = \pi/2$, where $t_B = 103\mu s$. Once the Bragg pulse splits the BEC into condensates of two momentum states of equal population, an AOKR kicking pulse is applied to create the ratchet steps. The average momentum shifted by the action of a pulse of the AOKR and is given by,

$$\langle \Delta p \rangle = -\frac{\phi_d}{2}\sin(\phi) \tag{3.2.5}$$

By choosing $\phi = \pi/2$ and $\phi_d = 2$, the average momentum is either increased or decreased by one unit at each step of the walk depending on the sign of ϕ_d.

Experimentally, for ^{87}Rb, by choosing the frequency of the kicking laser pulse to equal the transition frequency from halfway between the $5^2S_{1/2}$, F=1 and F=2 to the $5^2P_{3/2}$, F'=3 excited state, the laser frequency is equally detuned from the transition from the F=1 and F=2 states to the excited states by exactly $\pm 3.4\ GHz$. From theory, $\phi_d \propto \frac{1}{\delta_L}$ and hence, the atoms in both these states experience the same amount of kicking but in the opposite direction forming a sate dependent ratchet. The kick operator is given as,

$$\widehat{K} = e^{-i\phi_d[1+cos(\hat{x})]\sigma_z} = \begin{pmatrix} e^{-i\phi_d[1+cos(\hat{x})]} & 0 \\ 0 & e^{i\phi_d[1+cos(\hat{x})]} \end{pmatrix} \tag{3.2.6}$$

Where the diagonal elements of the matrix address the internal states of the condensate. The operator when used in the ratchet configuration shifts the momentum in integer units of $\hbar G$.

To obtain an initial system with equal population in the two internal states $5^2S_{1/2}$, F=1 and F=2, microwave (MW) radiation is used. The unitary operator of a MW pulse is derived in [18] and has a similar form as that of Eq. (3.2.4),

$$\widehat{M}(\theta(t), \chi) = \begin{pmatrix} \cos\left(\frac{\theta(t)}{2}\right) & e^{i\chi}\sin\left(\frac{\theta(t)}{2}\right) \\ -e^{i\chi}\sin\left(\frac{\theta(t)}{2}\right) & \cos\left(\frac{\theta(t)}{2}\right) \end{pmatrix} \tag{3.2.7}$$

where $\theta(t) = \Omega \cdot t$, Ω is the Rabi frequency, t is the pulse duration, and χ is the offset phase of the resonance pulse. To get equal population in the two initial states, a $\pi/2$ pulse ($\theta(t) = \Omega \cdot t = \pi/2$) is applied to get the following operator,

$$\widehat{M}(\pi/2, \pi) = \frac{1}{\sqrt{2}}\begin{pmatrix} 1 & -1 \\ 1 & 1 \end{pmatrix} \tag{3.2.8}$$

In the perspective of atom interferometry, the MW pulse behaves like a 50-50 internal state splitter that splits population from state $5^2S_{1/2}$, F=1 to $5^2S_{1/2}$, F=1 and F=2. Another MW pulse is used at the end of the interferometer to couple the atoms in the two states. By varying χ from 0° to 360°, we can see the effect of the atom interference.

CHAPTER IV

4. EXPERIMENTAL SETUP

The experimental setup needs to be capable of creation of the BEC, atom interferometry and atom detection. The formation of a BEC involves MOT creation, Doppler cooling, loading of dipole trap, and evaporative cooling. The BEC setup is divided into two optical tables, one for housing the lasers that will generate the required light for MOT creation, cooling and imaging and the other table for housing the BEC chamber and the CO_2 laser. The part of the lab that has the BEC chamber is isolated by using thick black curtains so as to minimize the light noise into the BEC chamber and to improve safety.

4.1. MOT Laser System

Four different laser frequencies are used in the experiment. Distinct frequencies are required for the MOT, Doppler cooling, imaging of the BEC, and repump. This capability is achieved by using two sets of lasers and optics known as the “Master” and the “Repump” lasers. The master is a grating stabilized TOPTICA, DL100 laser in a temperature-controlled housing. This laser has an output power of 20 mW output power in the CW mode and is frequency locked to the transition between F=2 ground state and the cross over line between F’=2 and F’=3 excited states as shown in Figure 5.

The Master laser is then used to injection lock three more lasers (called the "slave" lasers) for amplification of the laser beam as the power of the master laser is too low. For laser cooling, each of the slave lasers used has an output power of 100mW in the CW mode and is mounted in a temperature controlled housing. When the injection beam from the Master laser is properly aligned, the modes of slave matches the master at certain current and temperatures.

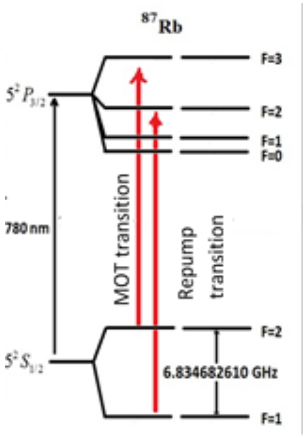

Figure 5: Hyperfine energy levels of ^{87}Rb indicating the MOT and the repump transition[14]

The collimated output from the laser diode is elliptical in shape. To make the beam circular, the laser beam is passed through a pair of anamorphic prisms. The polarization of the light is modified using a half wave plate so as to pass through a polarizing beam splitter cube (PBSC). The light is then passed through a Faraday rotator making it horizontally polarized. A PBSC is then placed in so that the horizontally polarized light is transmitted and if there are any back reflected beams through the PBSC, the light is eliminated by the isolator before the laser cavity. This makes sure that the master laser is isolated from any incoming back reflected beams.

To lock the laser frequency, saturation absorption spectroscopy is done using a small portion of light from the master laser. The rest of the light (about 10 mW) is sent into the next slave laser for injection-locking. In order to make sure all lasers are following the master laser, small portions of their output is passed through a ^{87}Rb vapor cell and then to a photodiode to be able to see the absorption dip.

The master laser is locked at a frequency of 133 MHz below the MOT transition. This light is injection locked into a laser, called main slave, the output of which is double passed through an AOM (ISOMET 1205C-2). The double passing through the AOM is aided by a telescopic configuration of two lenses that retro-reflect the first order beam from the mirror so that they

propagate along the same path. This is a very important step in the optical configuration because three different frequencies are used to drive the AOM at different times and it is important for them to be in the same optical path so as to be able to use the same optics for all beams.

In order to have precise control over the laser frequencies, an acousto-optic modulator (AOM) is used between the master and the first slave. Its RF frequency is varied using a LabVIEW program which controls the voltage sent to a voltage controlled oscillator. The different frequencies required are:

- 20 MHz red-detuning from the F=2 to F'=3 transition to create the MOT
- 90 MHz red-detuning from the F=2 to F'=3 transition for Doppler cooling
- Resonant light for the F=2 to F'=3 transition for Imaging the BEC

The beam from the AOM is then injection locked into slave laser 1 and 15 mW of the output of slave laser 1 is injection locked into slave laser 2, for amplification. The output beam from the slave laser 1 and the rest of slave laser 2 is then sent together through another AOM (ISOMET 1205C-1) which is driven at frequency of 80 MHz. The negative first order is then used by splitting the beams using a PBSC and sent to the BEC optical table by using two polarization maintaining single-mode fibers referred to as fiber-1 and fiber-2. The final detuning from the $5^2S_{1/2}$, F = 2 to $5^2P_{3/2}$, F' = 3 transition achieved on the light entering the vacuum chamber can be calculated using the equation [4],

$$\delta = -133.3\ (MHz) + 2f_{AOM} - 80\ (MHz) \tag{3.1.1}$$

where $2f_{AOM}$ is the frequency added by the double pass AOM. This is adjusted to add 99.15 MHz, 66.5 MHz and 106.65 MHz to obtain -15 MHz, -80 MHz and 0 MHz required for MOT, Doppler Cooling and imaging respectively. The optical setup is shown in Figure 6.

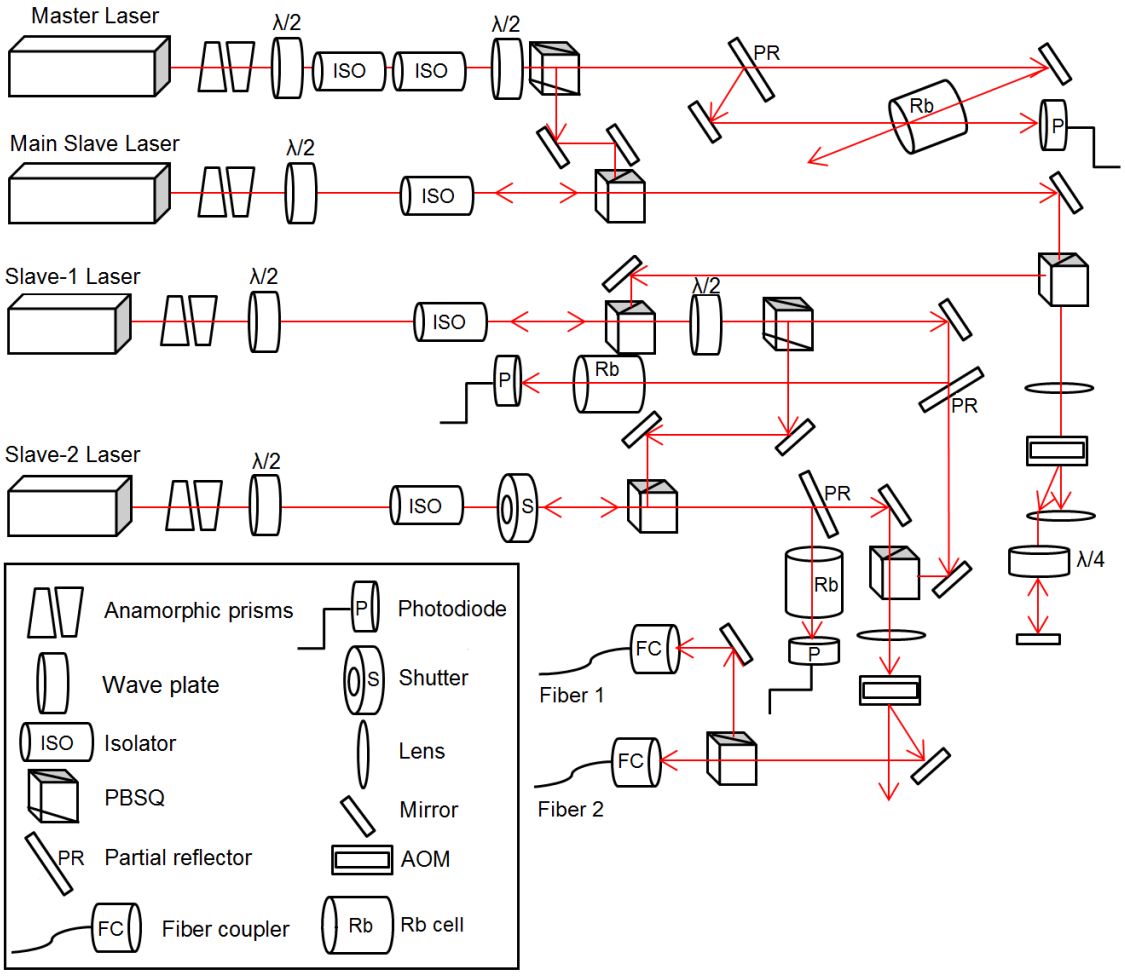

Figure 6: Optical setup to obtain frequency stabilized laser for MOT, Doppler cooling and Imaging[5]

4.2. Repump Laser System

Due to power broadening, there are always some atoms that decay into the $5^2S_{1/2}$, F=1 state. If the atoms continue to decay into this state, the MOT will disappear as the MOT is based on the $5^2S_{1/2}$, F=2 to $5^2P_{3/2}$, F'=3 transition. Hence, a grating stabilized TOPTICA, DL100 laser in a temperature controlled housing is used as a repump laser to put atoms back into the cycling transition. The different optical components used in this process is shown below in Figure 7.

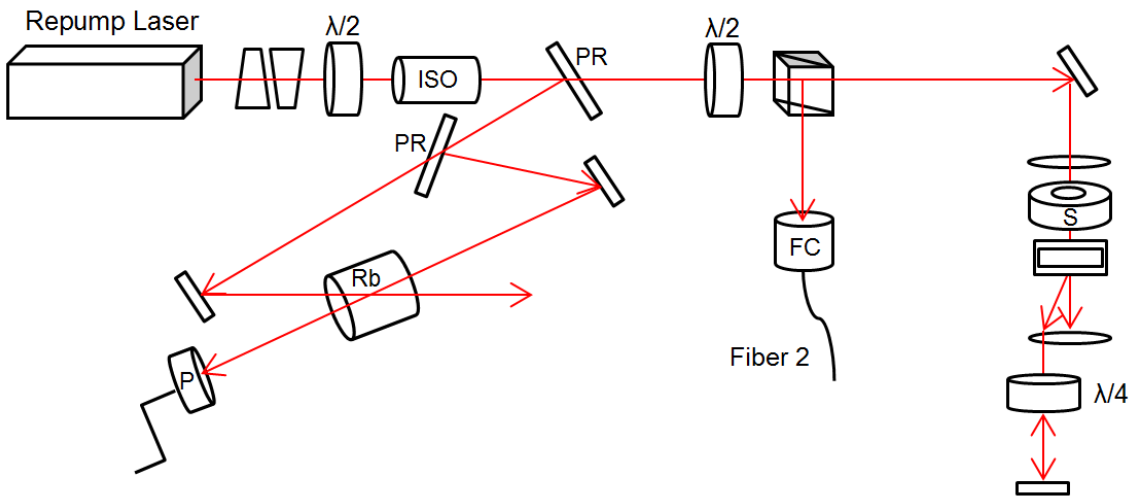

Figure 7: Repump Laser setup [5]

To complete the BEC creation process, the MOT beams and the repump laser beam, along with the evaporative cooling beam, needs to be transmitted into the vacuum chamber where the BEC will be generated. The MOT beam from fiber 1 and fiber 2 are split into 3 different beams and expanded to about 1 inch diameter by using two lenses and a quarter wave plate to make the light circularly polarized. These beams are sent into the vacuum chamber and are retro reflected using mirrors. To make sure they have the correct polarization, a quarter wave plate is used in between. The counter propagating beams are aligned to intersect at the center of the chamber where the MOT is formed. Figure 8 illustrates this process. During the experiment, the MOT, repump and imaging beams are blocked at various times depending on the stage of the experiment. This is done by using electronic shutters (UNIBLITZ, LS2T2) controlled by the LabVIEW program.

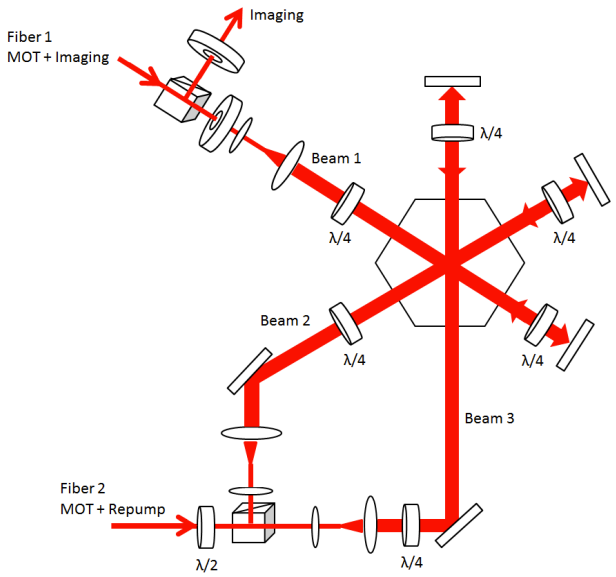

Figure 8: MOT, Doppler cooling, and Imaging beams in the Vacuum Chamber [5]

The magnetic field required for trapping of the atoms in the MOT is generated by a pair of current carrying coils in the anti-Helmholtz configuration (two identical coils separated by a distance equal to their radius, and currents flowing in opposite directions). The coil has a radius of 3.0 inches and consisted of 25 turns of copper with a square cross-section of external dimension 0.125 inch and internal dimension 0.016 inch. These coils are mounted around the large viewports of the vacuum chamber with their common axis along the symmetry axis of the chamber. In order to create the MOT, about 16 A current is supplied to produce a gradient magnetic field between the coils of 16 G/cm with a vanishing field at the center. This current through the coil is controlled with the LabView program by applying a 0-5 V analog signal to a 400 A DC current supply.

4.3. CO_2 Laser system

The laser in use is a Coherent, GEM Select-50 CO_2 laser powered by an Agilent, 6573A DC power supply, lasing at 10.6 μm wavelength. The 50 W laser source is used as a Far Off-

Resonant Trap (FORT) for evaporative cooling. Specialized optics made of Zinc Selenide (ZnSe) are used owing to its low absorption coefficient at 10.6 μm. Optics made from quartz and glass are not suitable for this purpose.

The FORT is passed through a water cooled AOM (IntraAction Corp., AGM 406-B1) driven by an IntraAction Modulator Driver Model GE-4030H which was electronically controlled by using an analog voltage signal controlled by the LabVIEW program. The zeroth order beam from the AOM is sent to a beam dump and the first order beam (30 W) is transported into the chamber through an assembly of three lenses. The first two lenses form a beam expander in a telescopic configuration followed by a third focusing lens (focal length = 1.5 inches) installed inside the vacuum chamber. The final spot size of the beam at the center of the chamber is $w_o = \frac{\lambda f}{\pi R}$ where R is the radius of the beam incident on the third lens and f is the focal length of the focusing lens. After loading into FORT, for the evaporative cooling, the beam waist (w_o) is reduced using the second lens of the beam expander. The second lens is mounted on a translation stage (Aerotech, 101SMB2-HM) controlled by a Soloist driver interface. The optics for the FORT are shown in Figure 9,

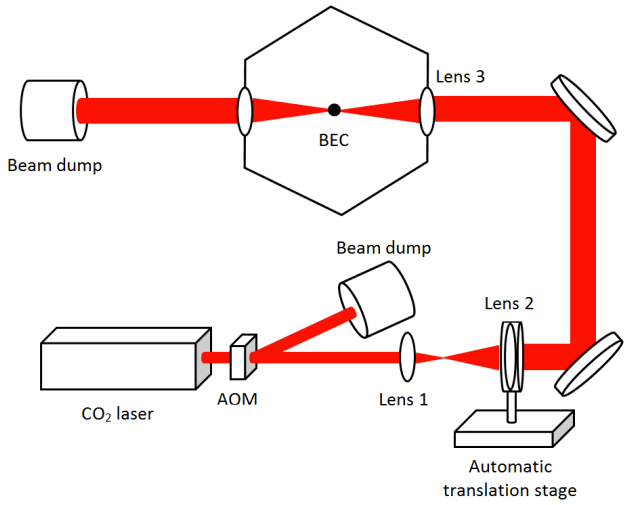

Figure 9: Optical setup for Far Off-Resonant Trap [5]

4.4. Vauum Chamber

The vacuum chamber is an integral part of the experiment where the BEC is created and manipulated. The vacuum system (from MDC Vacuum Products) is shown in Figure 10. The chamber has four antireflection coated quartz viewports (2 inches in diameter) for the MOT and kicking beams, four 1 inch diameter ZnSe viewports for CO_2 beam, and two 5 inch diameter quartz viewports (one attached to the open side of the six-way cross and the other attached to the large opening on the orthogonal chamber) used for MOT and imaging beams. The vacuum system is assembled and pumped in several phases to attain a vacuum of about 10^{-10} Torr. An automatic Varian style 8 liter/s ion pump powered by Terrenova-751 controller was attached to the system to keep the chamber at this pressure. The vacuum chamber is shielded from the magnetic field of the ion pump using μ-metal magnetic shields. Additionally, three pairs of coils are positioned on all six sides of the vacuum chamber to reduce the Earth's magnetic field and any stray field produced by other sources, mainly the ion pump. Each pair of coils has currents flowing in the same direction fed by a separate voltage-to-current converter circuit that is controlled through the LabVIEW program.

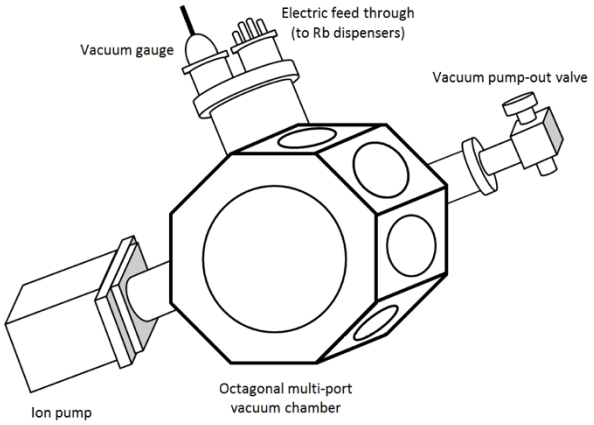

Figure 10: Vacuum Chamber [5]

4.5. Imaging System

A destructive absorption method is used to image the BEC. Recall that the BEC is created in $5^2S_{1/2}$, F=1. Once the BEC is formed, Experiments are done in terms of the perturbations on the atoms. The traps holding the atoms are turned off and the atoms are allowed to free fall in time-of-flight expansion for about 12 ms. Finally, to image the BEC, repump light is turned on so that the atoms are placed into the $5^2S_{1/2}$, F=2. During the time-of-flight expansion, the atoms are subjected to a pulse of imaging light. The imaging beam is in resonance with the transition from $5^2S_{1/2}$, F=2 to $5^2P_{3/2}$, F'=3. When exposed to a resonant light, the atoms scatter photons and cast a shadow, which is imaged by a high-resolution CCD camera (ANDOR DV437-BV). The operating temperature and the camera shutter time is controlled by the LabVIEW program. CCD cameras are also employed in monitoring the MOT in real time.

Due to absorption of the resonant light, the change in intensity (I) of the incident imaging beam in the z direction is given by,

$$\frac{dI}{dz} = -\sigma n I \tag{3.5.1}$$

where n is the number density of atoms and σ is the scattering cross-section. The intensity of the absorbed light is calculated by taking two images with and without atoms, where the intensity profile is given by the ratio of the intensities from the two images. The number of atoms (N) can then be calculated by integrating over the number of atoms per unit area,

$$N = -\frac{S}{\sigma} \sum_{pixels} \ln (I) \tag{3.5.2}$$

S is the scaled area of a pixel in the CCD camera (169 μm^2) and I is the ratio of the intensities.

4.6. Kicking Laser System

The kicking laser used is a grating stabilized TOPTICA, DL100 laser in a temperature controlled housing. This laser is set to operate at frequency equal to the transition frequency from halfway between the $5^2S_{1/2}$, F=1 and F=2 to the $5^2P_{3/2}$, F'=3 excited state. This is done so that the laser frequency is detuned from the transition from the F=1 and F=2 states to the excited states by exactly $\pm 3.4\ GHz$. As a result, the atoms in both these states experience the same magnitude kicking strengths.

A part of the beam from the main kicking laser is used to do the saturation absorption spectroscopy of 87Rb, and the rest of the beam is used for injection for injection into another slave laser, similar to the slave lasers of the MOT setup. This is done to amplify the kicking beam. The beam is then split in two and passed through two separate AOMs (ISOMET, 40N AOMs). The first order beam from the AOMs is then sent to the vacuum chamber, such that the beams make an angle of 53° with the vertical direction. At the intersection, a standing wave is formed with a spatial period $\lambda_S = \lambda/(2 \sin 53°)$, where λ is the wavelength of the kicking beam (~780 nm). The kicking laser setup is shown in Figure 11.

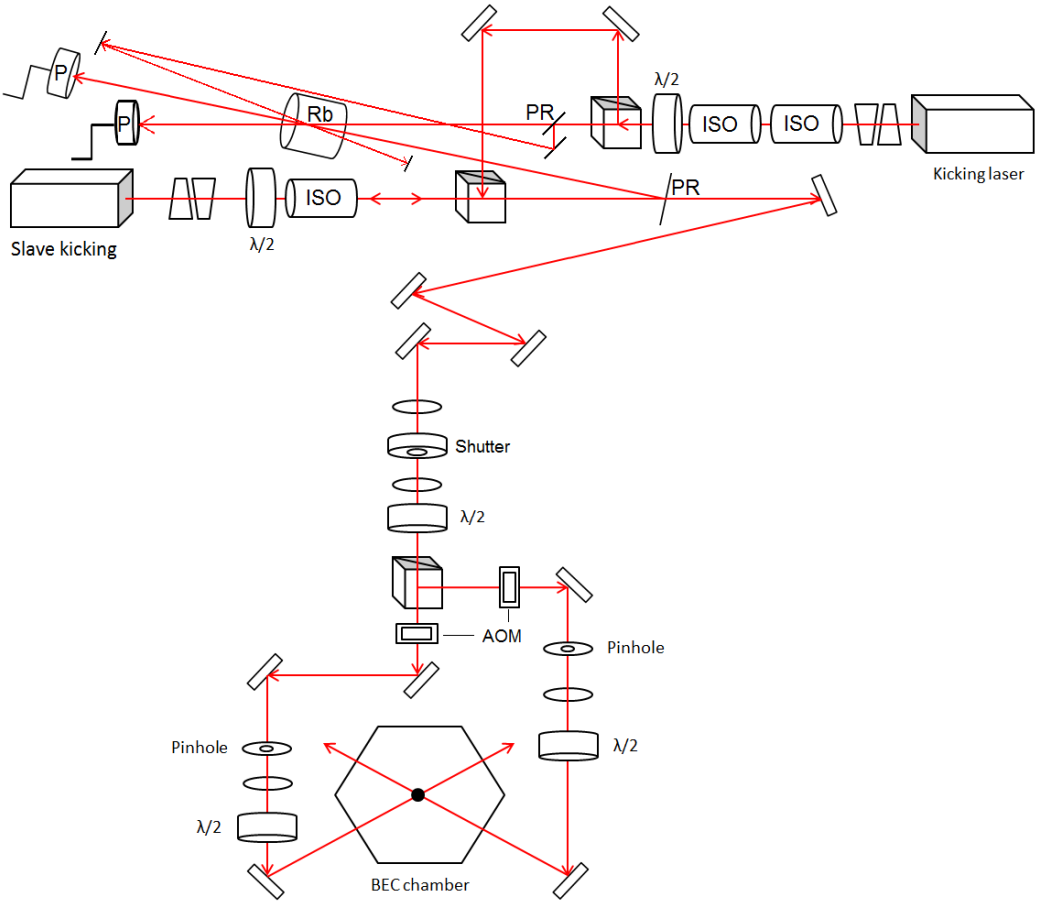

Figure 11: Kicking Laser Setup [5]

4.7. Microwave System

The MW pulses are generated by mixing a continuous MW signal of 6.8 GHz and an RF signal of frequency 34.682610 MHz. A Rb atomic clock is used to generate a 10 MHz reference for the 6.8 GHz crystal oscillator (Microwave Dynamics; PLO-4000) and the external clock for the programmable waveform generator (HP, HP8770A). The waveform generator synthesizes the RF pulses with the desired length, phase, and frequency. The waveform generator is also synched with the other kicking waveform generators to match the timing of each of the pulses.

The frequency generated is 6.834682610 GHz, which is the frequency of the $5^2S_{1/2}$, F=1 to $5^2S_{1/2}$, F=2 transition as shown in the Figure 12. The intensity of the MW radiation is controlled by adjusting the attenuation of the oscillator through the LabVIEW program. The output beam is amplified to about 30 dBm by a Terrasat Communications, ED-0278-4 amplifier and delivered to the vacuum chamber using a C-Band horn antenna. A schematic is shown in Figure 13.

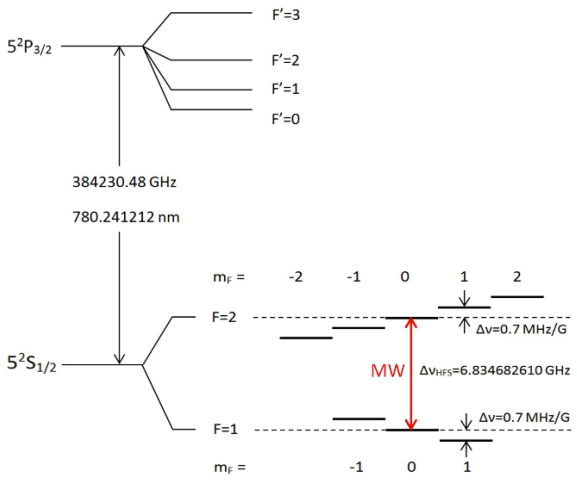

Figure 12: Hyperfine Structure of 87Rb with the Microwave transition between $5^2S_{1/2}$, F=1 to $5^2S_{1/2}$, F=2 [5]

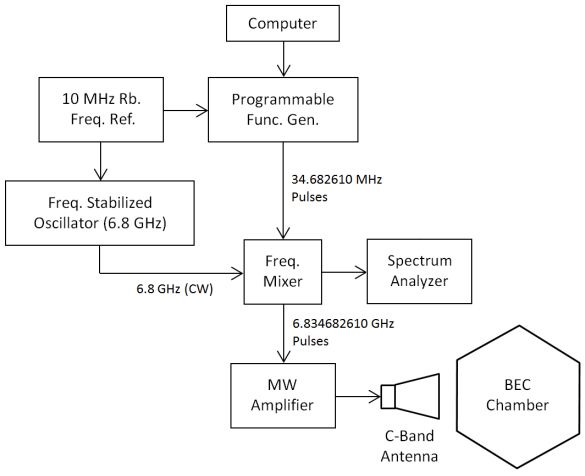

Figure 13: Schematic of the Microwave Setup [5]

CHAPTER V

5. EXPERIMENTAL CONFIGURATION AND RESULTS

A MOT is created by shining the MOT laser beams and the repump at the center of the vacuum chamber with the ^{87}Rb dispenser switched on. The MOT beam is -15 MHz detuned from the MOT transition and the repump is in resonance with the $5^2S_{1/2}$, F=1 to $5^2P_{3/2}$, F'=3 transition The MOT initially has about 30 million atoms. The CO_2 laser is then focused into the center of the chamber for about 15 seconds. The atoms are now loaded into the dipole trap (FORT). The power on the repump is reduced from 2.2 mW to create a temporal dark spot to reduce the recoil heating and excited state collisions and to increase the phase space density. The detuning on the cooling light is now increased to -80 MHz for the Optical Molasses (also known as Doppler cooling). About 100 ms later, the MOT beams and the repump is switched off. This reduces the number of atoms trapped to about 1 million. The FORT beam waist is reduced from about 100 μm to 25 μm to increase the elastic collision rates which is important for EVC. EVC is a 2 step process, the CO_2 laser power is decreased from 30 W to 2 W exponentially in 2 seconds. This is done by reducing the power given to the AOM controlling the first order beam. Then the power of the CO_2 laser is further reduced (at a slower rate), allowing for rethermalization. This is done over 5 seconds until the power is only about 50mW. This produces a BEC of about 80,000 atoms. The BEC is initially created in the $5^2S_{1/2}$, F=1 state. To image the BEC, the repump beam is applied followed by an imaging pulse.

By adjusting the power and the duration of the kicking light, different perturbations can be achieved. To get an initial state of a superposition of two momentum orders, a Bragg pulse is applied. The power of the kicking light determines the population in the two momentum orders and it is set to get equal population and the duration is set at 103 μs. Immediately after the Bragg pulse, a microwave pulse of duration 103 μs is applied. This ensures that half the population from $5^2S_{1/2}$, F=1 gets excited to $5^2S_{1/2}$, F=2. The microwave pulse is followed by a series of δ-kicks. As the name suggests, the kicks are light pulses that are of very short duration (0.384 μs) and a high kicking strength when compared to the Bragg pulse. A ratchet is achieved by repeating the kicks. The sequence of pulses to realize a ratchet with 5 number of kicks is shown in the Figure 14. The ratchet pulses can be continued for any number of required kicks. The experimentally realized ratchet is shown in Figure 15. After the Bragg pulse, the BEC starts as the superposition of the two momentum orders and the two arms of the ratchet correspond the atoms in either internal states of the ^{87}Rb.

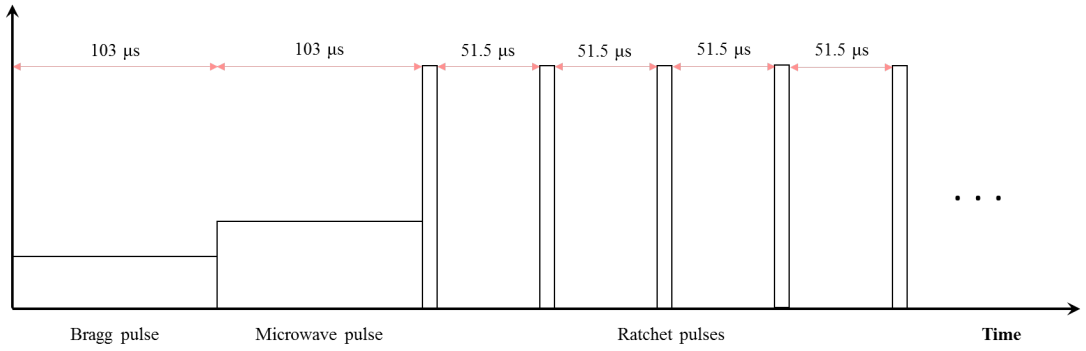

Figure 14: Sequence of pulses for realizing a bi directional ratchet. The pulse amplitudes are not to scale.

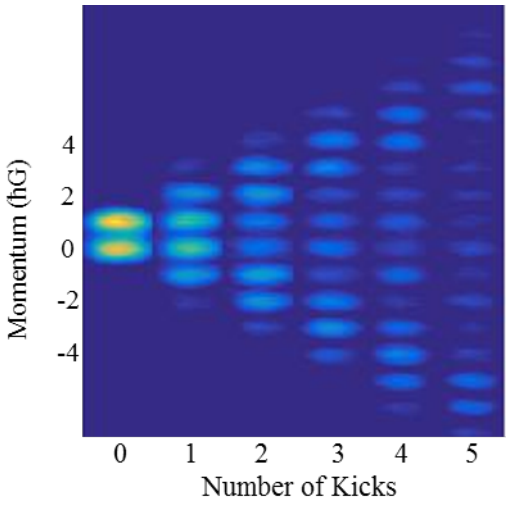

Figure 15: Experimental realization for a ratchet with 5 kicks.

The ratchet can be reversed by changing the offset phase of the kicking pulse by 180°. This makes the atoms move in the opposite direction such that the atoms can be brought back to let them interfere with each other. Required number of δ-kicks are applied to reverse the ratchet. The ratchet arms are analogous to the interferometer arms. A second microwave pulse, called the recombiner pulse, is applied at the end of the last δ-kick to complete the interferometer setup. The sequences of pulses for 2 kicks and 2 reverse kicks is shown in the Figure 16. Figure 17 shows the experimental realization of the reversed ratchet.

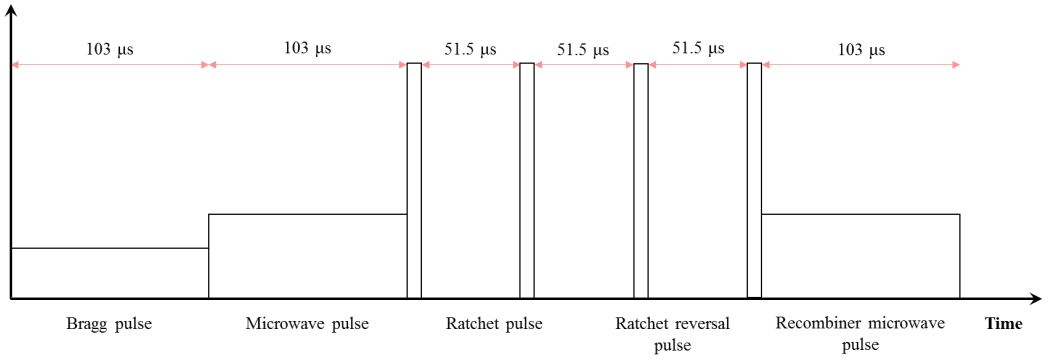

Figure 16: Sequence of pulses for producing a ratchet and then reversing it. The pulse ampklitudes are not to scale.

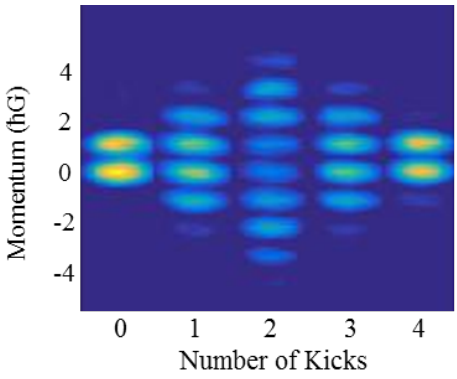

Figure 17: Experimental realization of the reversed ratchet with 2 ratchet steps and 2 reversal steps

The phase of the recombiner pulse is then scanned from 0° to 360°with an interval of 30° and the experimental result is shown in Figure 18. This is analogous to changing the phase of the one of the arms of the interferometer. A change in the population of the recombined condensate is shown as an intensity profile. The intensity of the number of atoms in the beginning of the scan is low, indicating a lower population of atoms in the F=2 state. As we keep scanning, the population in the F=2 state increases and then becomes low again in a periodic fashion.

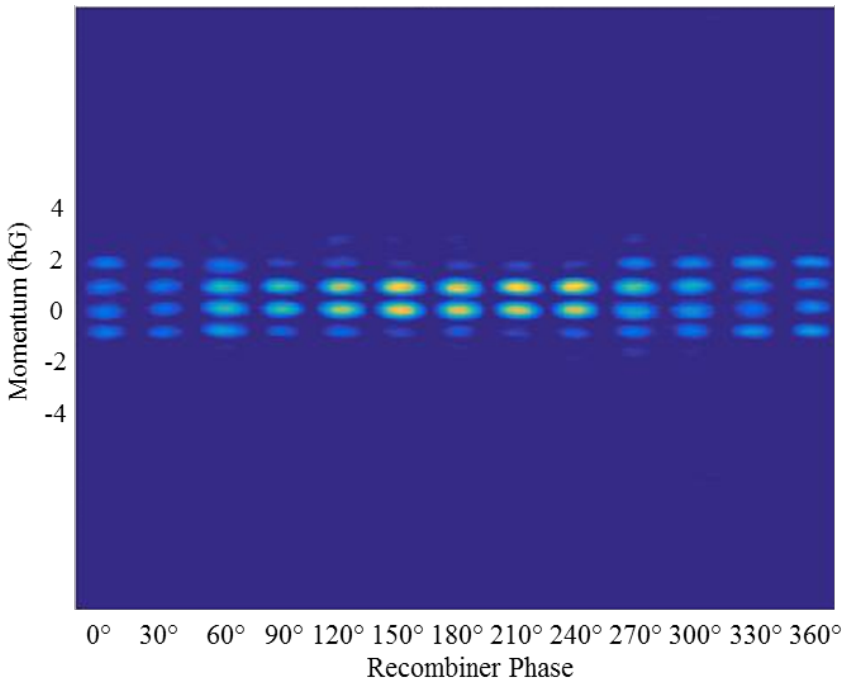

Figure 18: Population variation in the internal state, $5^2S_{1/2}$, F=2, in the final step of the reversed ratchet with 2 kicks scanned from 0° to 360° with an interval of 30°, identified through the change in intensity

This demonstrates a working atomic interferometer. The complexity of the interferometer can be increased by increasing the number of kicks. The experimented is repeated by performing 3 ratchet steps and 3 reversal steps and the phase of the recombiner pulse is again scanned from 0° to 360°, with an interval of 30°. The results of the ratchet and the phase scan are shown in Figure 19 and Figure 20 respectively.

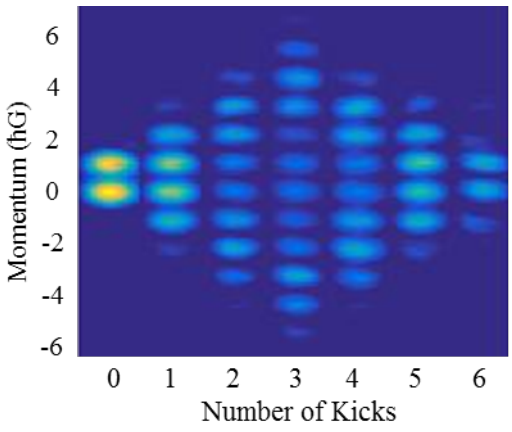

Figure 19: Experimental realization of a reversed ratchet with 3 ratchet steps and 3 reversal steps

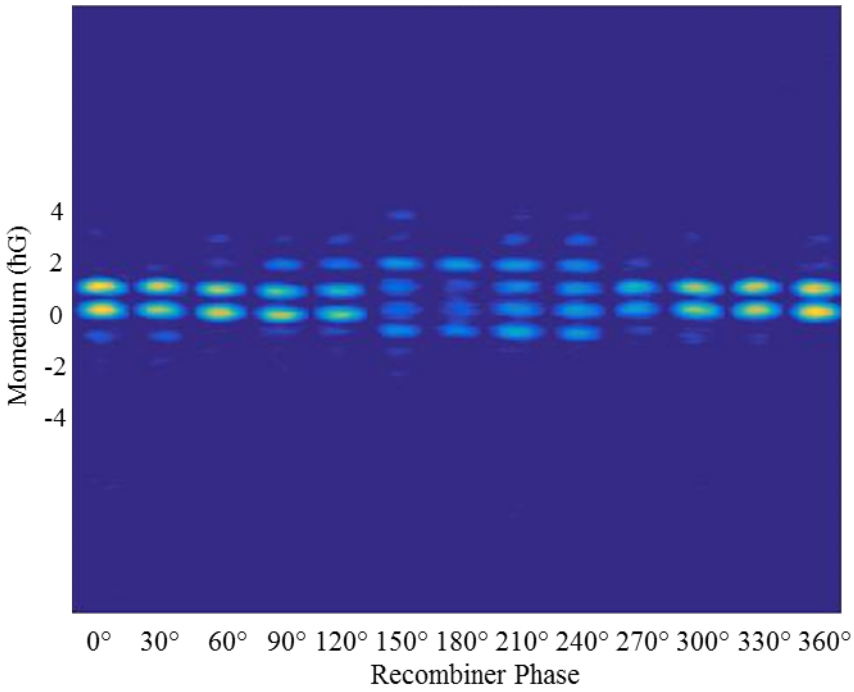

Figure 20: Population variation in the internal state, $5^2S_{1/2}$, F=2, in the final step of the reversed ratchet with 3 kicks scanned from 0° to 360° with an interval of 30°, identified through the change in intensity

It is interesting to note that the phase scan shifts by 180°. To investigate this further and to check the accuracy of the MW setup, the two experiments from above were repeated but without any kicking light. In this sequence of the experiment, the BEC is illuminated with just the two MW pulses and are shown in Figure 21. If the MW pulse generated is at the right frequency, we would see the same behavior of the change in population as the regular configuration of the experiment.

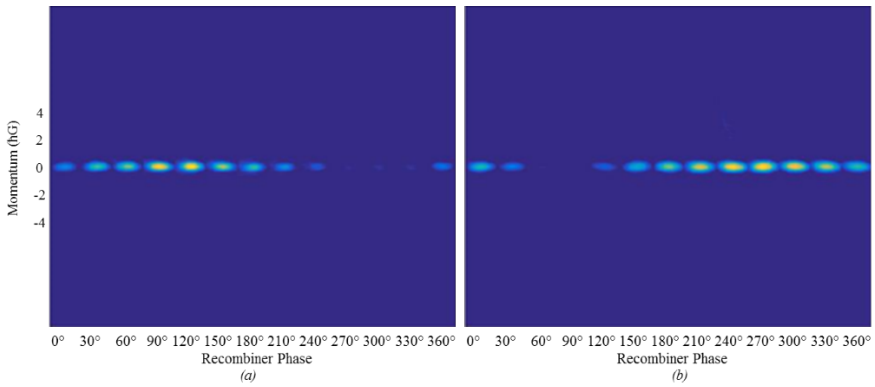

Figure 21: Population variation in the internal state, $5^2S_{1/2}$, F=2, when two MW pulses are applied, scanned from 0° to 360° with an interval of 30°. Identified through the change in intensity (a) The time between pulses are the same as that of an experiment with 2 reversed ratchet kicks. (b) The time between pulses are the same as that of an experiment with 3 reversed ratchet kicks.

The results show that there is about a 180° shift in the fringe pattern. This implies that the MW frequency is not exactly equal to the $5^2S_{1/2}$, F=1 to $5^2S_{1/2}$, F=2 transition. The detuning in the MW radiation from the $5^2S_{1/2}$, F=1 to $5^2S_{1/2}$, F=2 transition can be calculated from the following equation,

$$\Delta\omega \cdot \Delta t = \Delta\phi$$

where $\Delta\omega$ is the detuning in the frequency, Δt is the difference in the time between pulses in the two cases and $\Delta\phi$ is the phase difference between the minima and the maxima in the two fringe patterns. From the equation, the frequency detuning is calculated to be 30.35 kHz or an odd multiple of the same. Another observation is that the maxima in the fringe pattern between the experiments with and without the kicking light has shifted by about 90°. This is due to not compensating for the global phase (equal to $2\phi_d$) imparted by the kicking pulse from Eq. (3.1.2).

The global phase is a manifestation of the light (ac-Stark) shift. This can be compensated by adding it to the offset phase of the MW pulse.

The experiment was also performed with 4 ratchet steps and 4 reversal steps and the phase of the recombiner microwave pulse is again scanned from 0° to 360°with an interval of 30°. The result is shown in Figure 21. Although the result is noisy, the scan seems to follow the behavior seen in the case with 2 ratchet steps and 2 reversal steps.

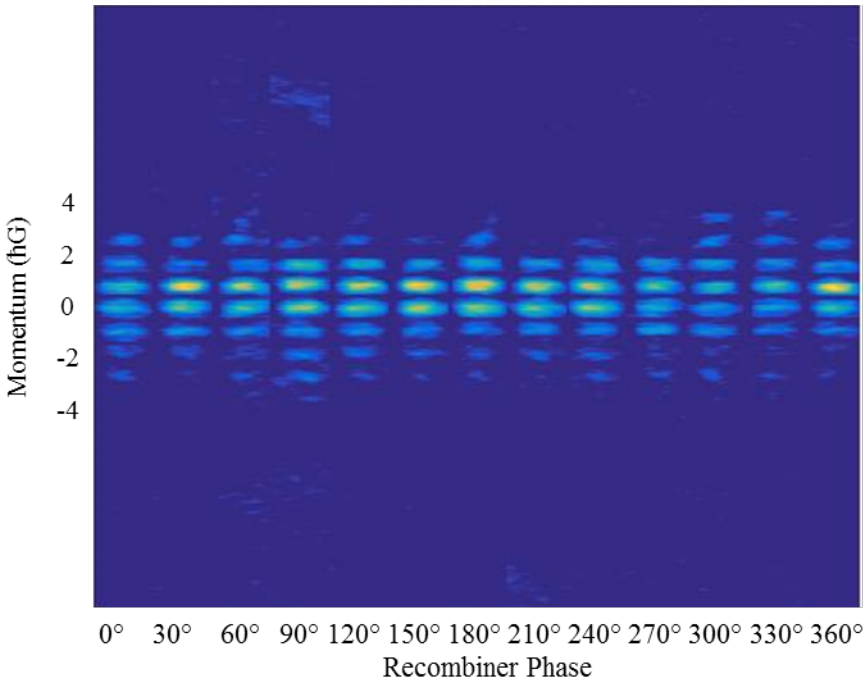

Figure 22: Population variation in the internal state, $5^2S_{1/2}$, F=2, in the final step of the reversed ratchet with 4 kicks scanned from 0° to 360° with an interval of 30°, identified through the change in intensity.

CHAPTER VI

6. CONCLUSION AND FUTURE IMPROVEMENTS

An atom interferometer in a BEC ratchet is demonstrated with 2 ratchet steps and 2 reversal steps by scanning the phase of the recombiner microwave pulse from 0° to 360° with an interval of 30°. The number of atoms in the $5^2S_{1/2}$, F=2 state of the ^{87}Rb is observed to periodically change with a change in the phase of the recombiner pulse. The experiment is repeated for 3 ratchet steps and 3 reversal steps. The results for both the cases are shifted by 180°. The shift is attributed to the inaccuracy of the frequency of the MW pulse.

This phenomenon can be further investigated by optimizing the experiment to reduce the noise detected in experiments with higher number of kicks and a higher kicking strength. The experiment can also be repeated with a change in the time between pulses of the ratchet steps. A magnetic field gradient can be applied to investigate the Zeeman and the second order Zeeman shift during the interferometer action. The interferometer can be realized using a sequence of Quantum Random Walk (QRW) steps instead of ratchet steps.

REFERENCES

[1] Alexander D. Cronin, Jörg Schmiedmayer, and David E. Pritchard, *Optics and interferometry with atoms and molecules*, Rev. Mod. Phys. 81, 1051 (2009)

[2] Alexander D. Cronin, *Viewpoint: More Power to Atom Interferometry*, Physics 8, 22.

[3] Z C Tu, *Efficiency at maximum power of Feynman's ratchet as a heat engine*, Journal of Physics A: Mathematical and Theoretical, Volume 41, Number 31.

[4] R. K. Shrestha, *Applications of the atom-optical kicked rotor*, Doctoral thesis, Oklahoma State University, May 2013.

[5] Siamak Dadras *, Discrete-Time Quantum Walk Of A Bose-Einstein Condensate In Momentum Space* Doctoral thesis, Oklahoma State University, April 2013.

[6] I. Dana, V. Ramareddy, I. Talkukdar, and G. S. Summy, *Experimental realization of quantum-resonance-ratchets*, Phys. Rev. Lett. 100, 024103 (2008).

[7] Jiating Ni, Siamak Dadras, Wa Kun Lam, Rajendra K. Shrestha, Mark Sadgrove, Sandro Wimberger, and Gil S. Summy, *Hamiltonian Ratchets with Ultra-Cold Atoms*, Ann. Phys. (Berlin) 2017, 529, 1600335.

[8] I. Dana and V. Roitberg, *Quantum resonances and ratchets in freely-falling frames*, Phys. Rev. E. 76, 015201(R) (2007)

[9] P. D. Lett, R. N. Watts, C. I. Westbrook, W. D. Phillips, P. L. Gould, and H.J. Metcalf, *Observation of Atoms Laser Cooled below the Doppler Limit*, Phys. Rev. Lett. 61, 169 (1998).

[10] W. D. Phillips, *Nobel Lecture: Laser Cooling and Trapping of Neutral Atoms*, Rev. Mod. Phys. 70, 721 (1998).

[11] P. L. Gould, P. D. Lett, and W. D. Phillips, *New Measurements with Optical Molasses*, in Laser Spectroscopy VIII, (SpringerVerlag, Berlin 1987).

[12] Harold J. Metcalf and Peter van der Straten, *Laser Cooling and Trapping*, (Springer 1999).

[13] L. E. Reichl, *The Transition to Chaos*, 2nd ed.(Springer, New York, 2004).

[14] Siamak Dadras*, Investigation of Quantum Fidelity Using δ-Kicked Rotor in Ramsey Interferometry of ^{87}Rb Cold Atoms*, Report for the PhD Qualifying Exam, Oklahoma State University, Dec 2015.

[15] Summy, G and Wimberger, S, *Quantum random walk of a Bose-Einstein condensate in momentum space,* Physical Review A 93, 023638 (2016).

[16] Liang Hu, Nicola Poli, Leonardo Salvi, and Guglielmo M. Tino, *Atom Interferometry with the Sr Optical Clock Transition,* Phys. Rev. Lett. 119, 263601 (2017)

[17] Matthias Weidemüller and Claus Zimmermann, *Interactions in Ultra Cold Gasses: From Atoms to Molecules* (John Wiley & Sons, 2011)

[18] S. Kuhr, *A controlled quantum system of individual neutral atoms*, Doctoral thesis, Bonn University, 2003.

VITA

Amruthaa Sundararaj

Candidate for the Degree of

Master of Science

Thesis: ATOM INTERFEROMETRY IN A BOSE-EINSTEIN CONDENSATE RATCHET

Major Field: Physics

Biographical:

Education:

Received the Bachelor of Technology in Nanotechnology from SRM University, Chennai, India in 2015

Completed the requirements for the Master of Science in Physics, Photonics Option at Oklahoma State University, Stillwater, OK in 2018.